Performance of a low-pass filter for far-infrared wavelengths

J. J. Bock and A. E. Lange

We describe a low-pass filter that provides high in-band transmittance and excellent rejection at $\nu > 100$ cm^{-1}. The transmittance of the filter components was measured at liquid-helium temperatures from 10 to 10,000 cm^{-1}. The total transmittance is >50% for $\nu < 50$ cm^{-1} and is calculated to be $<10^{-9}$ for $\nu > 300$ cm^{-1}. The filter was successfully used in a liquid-helium-cooled, rocketborne, far-infrared absolute photometer.

Key words: Far-infrared, low-pass filter, spectroscopy.

1. Introduction

Spaceborne, far-infrared photometry is complicated by the relative brightness of the zodiacal light in the mid-infrared and the near-infrared. Because far-infrared detectors, particularly bolometers, are generally sensitive to high-frequency radiation, it is necessary to use a low-pass filter to attenuate the high-frequency response strongly. The requirements for high-frequency blocking are severe, as the sky in the mid-infrared and the near-infrared is orders of magnitude brighter than it is in the far-infrared.

We have developed an absorbing, low-pass filter suitable for use in absolute spaceborne observations that combines both ionic salts and carbon in polyethylene to achieve rejection across a broad range of frequencies. Yoshinaga filters consisting of ionic salts embedded in polyethylene[1] and polyethylene filters loaded with carbon[2] are often used as low-pass filters in far-infrared spectroscopy. Ionic salts are most useful in blocking mid-infrared and far-infrared radiation, whereas carbon-loaded filters are most efficient in blocking mid-infrared and near-infrared radiation. Our filter is easy to fabricate and to mount, and it is robust to mechanical and thermal shock. It was used in a liquid-helium-cooled, rocketborne, far-infrared absolute photometer designed to measure the far-infrared continuum and the 158-μm line emission from singly-ionized carbon.[3–5]

The authors are with the Department of Physics, California Institute of Technology, Pasadena, California 91125.

Received 18 April 1995; revised manuscript received 20 July 1995.

0003-6935/95/317254-04$06.00/0.

2. Measurements

The low-pass filter comprises two components: two 360-μm sheets of a low-pass filter with a stop band ($T < 0.1$) beginning at approximately 100 cm^{-1} (LP100) and one 245-μm sheet of a low-pass filter with a stop band beginning at 250 cm^{-1} (LP250). The formulation of the LP100 filter was developed by Perkin Elmer[6] for use in a far-infrared spectrometer. We manufactured each component of the low-pass filter by grinding the ionic salts and carbon lampblack into a fine powder; the relative amounts of each are listed in Table 1. Diamond powder is added after these ingredients are ground. The salts, diamond powder, and carbon lampblack are then thoroughly mixed with powdered polyethylene and placed between two Mylar sheets. A spacer is inserted between the Mylar sheets to control the thickness of the filter. The Mylar sheets, spacer, and powdered mixture are placed between the platens of a laboratory press. The platens are heated to 100 °C by an electric heater, melting the polyethylene. After the polyethylene melts, the platens are closed with 100 MPa of pressure and are permitted to cool to room temperature to produce a single filter.

We measured the transmittance by placing the filters in an $f/3.5$ light pipe at the output of a Fourier-transform spectrometer, as shown in Fig. 1. The transmittance of Yoshinaga filters is known to change on cooling to cryogenic temperature.[7] Therefore, to ensure that the filters remain at liquid-helium temperature in the presence of large optical heating, the filters are immersed in superfluid helium. A composite bolometer[8] positioned in a vacuum cavity behind an $f/1.6$ Winston concentrator[9] and two filter wheels is used to measure the transmittance. The spectral coverage is selected by a fixed, low-pass filter

Table 1. Composition of the Low-Pass-Filter Components

Filter	Composition	Ingredients	Stop Band[a]
LP100[b]	1000 mg	Polyethylene[c]	
	300 mg	Calcium carbonate	90–135
			185–245
			270–450
			700–1800
	200 mg	Potassium chloride	125–230
	120 mg	Magnesium oxide	475–780
	40 mg	Barium fluoride	170–260
	40 mg	Beryllium oxide	625–1100
LP250	1000 mg	Polyethylene	
	200 mg	Diamond powder[d]	>525
	100 mg	Lithium fluoride	300–640
	25 mg	Carbon lampblack[e]	>575

[a]The values represent the approximate measured stop band(s) ($T < 0.1$) for each ingredient.
[b]Formerly filter 180-1048 from Perkin-Elmer, Inc.
[c]Obtained from the Aldrich Chemical Co. Inc., Milwaukee, Wis. 53233, catalog no. 26,935-2 in 1993.
[d]Obtained from Carbide Products Co. Inc., Torrance, Calif., 90501, size 9.
[e]Obtained from Fisher Scientific, Inc., Pittsburgh, Pa. 15219, catalog no. C198-500 in 1995.

placed in front of the bolometer and by low-pass filters placed on the upper filter wheel.

The transmittance spectrum obtained with the filter inserted in the optical path is normalized to that obtained with an open aperture. We check for any leaks in the optical system by routinely measuring the transmittance of a closed aperture. Several measurements were made with different bolometers that had been constructed for optimum sensitivity under the background loading present in a given spectral range. The responsivity of the bolometer was monitored during the measurement and did not change by more than 5% when the samples under test were inserted in the optical path. The in-band transmittance of the two filters is shown in Fig. 2.

Because of the practical difficulty of measuring the high-frequency blocking of the filter stack directly, we measured the transmittance of the components separately. In addition, we measured several thicknesses of each component to probe the absorptivity at frequencies for which the transmittance was below the sensitivity of the instrument. The transmittances of the LP100 and LP250 samples are shown in Fig. 3. The minimum measurable transmittance is defined to be 3 times the statistical rms deviation, as calculated from transmittance spectra of the closed aperture. To confirm that the filters did not have pinholes, we measured the optical transmittance at room temperature with a photodiode and a lamp. The optical transmittance of a 100-μm-thick LP250 filter is $T < 10^{-7}$.

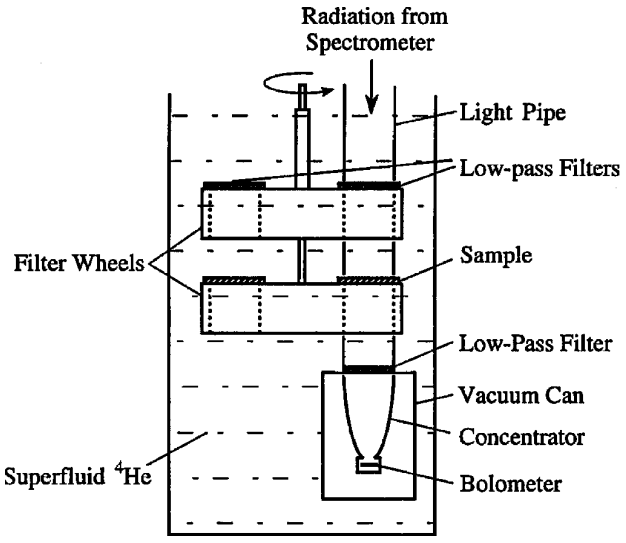

Fig. 1. Schematic diagram of the instrument used to measure the transmittance of the filters. Radiation from the Fourier-transform spectrometer is coupled into a light pipe, passes through two filter wheels, and is concentrated onto a bolometer. The apparatus is immersed in superfluid ^{4}He, except for the bolometer and the concentrator, which are housed inside an evacuated can sealed against the liquid helium by a polypropylene window. The spectral coverage is selected by a fixed low-pass filter placed in front of the bolometer and by low-pass filters placed on the upper filter wheel.

3. Discussion

The filters attenuate radiation by absorption in the reststrahlen bands of the ionic salts and by absorption caused by the carbon-lampblack particles. High-frequency radiation, when the wavelength is of the order of the particle size or smaller, will be strongly scattered by the powdered ingredients. If the attenuation is entirely due to absorption, then the transmittance of the filter is given by

$$T \approx (1 - R_n)^2 \exp(-\alpha t), \quad (1)$$

where α is the absorption coefficient, t is the thickness of the sample, R_n is the surface reflection, and the

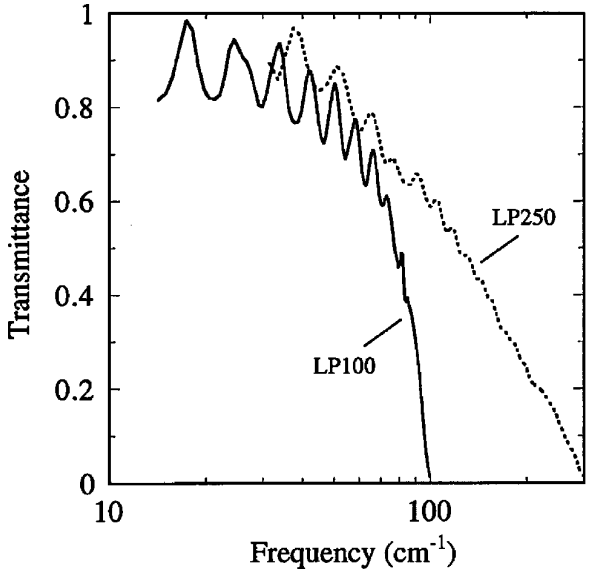

Fig. 2. Plot of the in-band transmittance of a 360-μm-thick sample from a LP100 filter (solid curve) and from a 245-μm-thick sample from a LP250 filter (dotted curve).

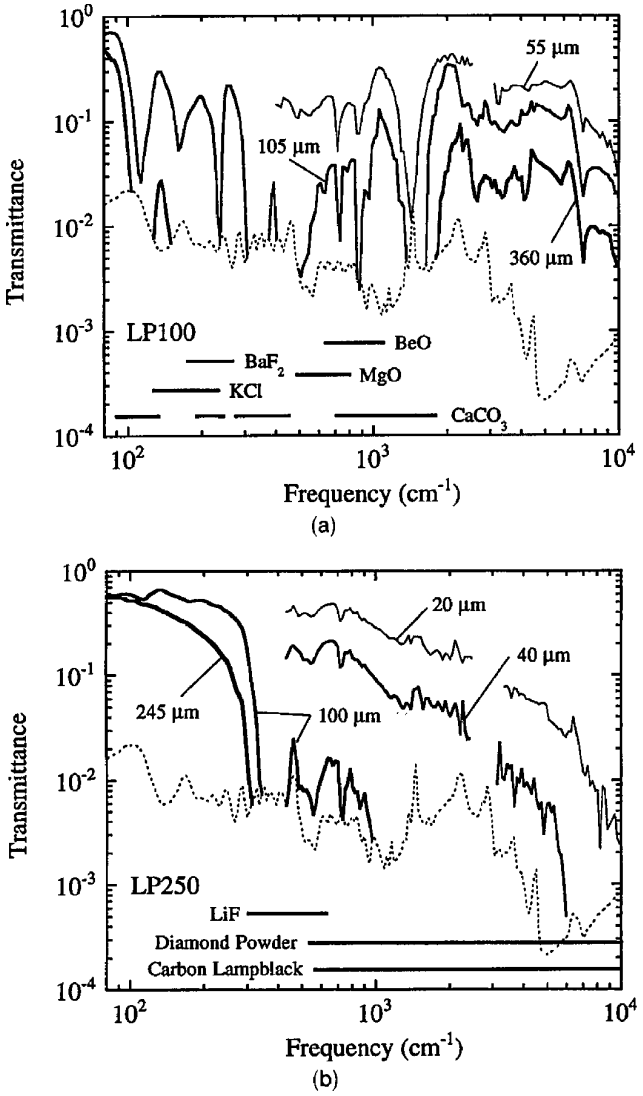

Fig. 3. Plots of the out-of-band transmittances measured at superfluid-helium temperatures of (a) 55-, 105-, and 360-μm-thick samples from the LP100 filter, and (b) 20-, 40-, 100-, and 245-μm-thick samples from the LP250 filter. The data were obtained when multiple measurements are co-added into logarithmic frequency bins [$\Delta \log_{10}(\nu) = 0.01$]. The minimum measurable transmittance, indicated by the dotted curve, is defined to be 3 times the statistical rms deviation in each frequency bin from the measurement of the closed aperture. The solid horizontal lines at the bottoms of the graphs indicate the bands of frequencies over which each of the filter components provides significant blocking.

small effect of Fabry–Perot fringing has been neglected. By comparing the spectra of several sample thicknesses we can thus determine if the transmittance scales exponentially with the thickness of the sample, as is expected for an absorbing filter, or if it scales less strongly with the sample thickness, as is expected for a scattering filter.

The transmittance of the LP250 filter scales exponentially with thickness, indicating that absorption dominates over scattering. The transmittance of the LP100 filter, however, is clearly dominated by scattering at high frequencies. For example, the transmittance of the 105-μm-thick LP100 sample is $T \sim 0.1$ at both $\nu = 1000$ cm^{-1} and $\nu = 3000$ cm^{-1}. However, the transmittance of the 360-μm-thick sample is $T < 2 \times 10^{-3}$ at $\nu = 1000$ cm^{-1} but is much higher, $T = 2.5 \times 10^{-2}$ at $\nu = 3000$ cm^{-1}. The onset of scattering in the LP100 filter occurs at $\nu > 1800$ cm^{-1}, which corresponds to frequencies higher than the highest-frequency ($CaCO_3$) reststrahlung absorption band.

We calculate the high-frequency rejection of the filter stack by extrapolating the measured transmittance of the thinner samples using Eq. (1) at frequencies at which the transmittance of the thick samples is below the instrument noise and then by multiplying the transmittances of the two components. We constrain the term $(1 - R_n)^2$ by assuming $R_n < 0.1$, which was confirmed by room-temperature measurements of the reflectance of the filters. We use the measured transmittance of a single 360-μm-thick LP100 sample at $\nu > 1800$ cm^{-1} as an upper limit on the transmittance of the LP100 component at high frequencies when scattering dominates over absorption. The out-of-band rejection of the low-pass filter stack calculated in this manner is shown in Fig. 4. The in-band transmittance of the low-pass filter stack is $T > 50\%$ for $\nu < 50$ cm^{-1}. The calculated out-of-band rejection is $T < 10^{-9}$ for $\nu > 300$ cm^{-1}.

For a given passband, the out-of-band transmittance shown in Fig. 4 can be used to estimate the relative contribution from in-band and out-of-band power. For example, in Fig. 5 we multiply the transmittance of the low-pass filter by the brightness of a region of the astrophysical sky with low galactic emission that is viewed at a large solar elongation.[3,10] The calculated out-of-band leakage is concentrated at low frequencies. For example, the integrated out-of-band power for 100 cm$^{-1} < \nu < 300$ cm^{-1} is $\geq 7 \times 10^4$ times the out-of-band power for 300 cm$^{-1} < \nu <$

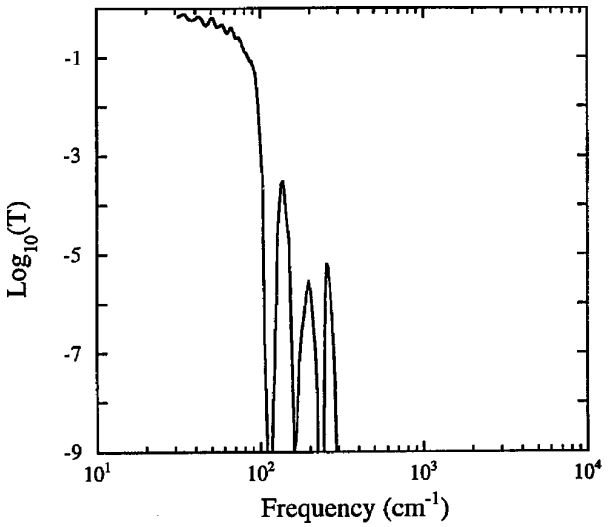

Fig. 4. Calculated transmittance of a low-pass filter stack consisting of two 360-μm sheets of the LP100 component and one 245-μm sheet of the LP250 component. The transmittance is $<10^{-9}$ for $\nu > 300$ cm^{-1}.

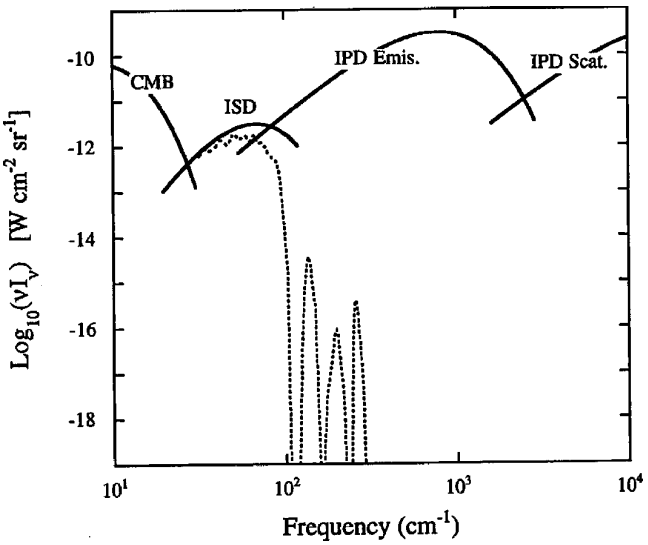

Fig. 5. Spectral brightness spectra (solid curves) of a region of the astrophysical sky with low galactic emission that is viewed at a large solar elongation. In order of increasing frequency, the brightness is dominated by the cosmic microwave background (CMB), thermal emission from interstellar dust (ISD), and thermal emission and scattering by interplanetary dust (IPD). The ISD spectrum is scaled to a region that had a neutral hydrogen column density, $N_{HI} = 1 \times 10^{20}$ cm^{-2}, as determined from an observation at a high galactic latitude.[3] The IPD spectra were taken from an observation of the astrophysical sky brightness at the south ecliptic pole.[10] The sky brightness multiplied by the transmittance of the low-pass filter stack is indicated by the dashed curve.

10,000 cm^{-1}. The level of out-of-band leakage for a given experiment will depend on the characteristics of the detector, on additional filtering to define a passband, and on the region of the astrophysical sky under observation. For example, assuming a $\Delta\nu/\nu = 20\%$ passband centered at 50 cm^{-1} with no additional filtering, we calculate that the total out-of-band power is $<1.3 \times 10^{-3}$ of the in-band power. Additional blocking by other filter components at 110 cm$^{-1} < \nu < 300$ cm^{-1} will further improve the high-frequency rejection. The in-band transmittance may be increased at the expense of high-frequency rejection by a decrease in the quantity of the LP100 component.

4. Conclusion

We have measured the transmittance of a low-pass filter that provides a high degree of out-of-band rejection, enabling the accurate absolute photometry of the astrophysical sky at far-infrared wavelengths.

The authors thank P. L. Richards for the use of his spectrometer. The details of the LP100 filter were kindly provided by M. T. Stier. The authors acknowledge support by NASA under grants NAGW-1352 and NGT-50771.

References and Notes

1. Y. Yamada, A. Mitsuishi, and H. Yoshinaga, "Transmission filters in the far-infrared region," J. Opt. Soc. Am. **52,** 17–19 (1962).
2. J. M. Blea, W. F. Parks, P. A. R. Ade, and R. J. Bell, "Optical properties of black polyethylene from 3 to 4000 cm^{-1}," J. Opt. Soc. Am. **60,** 603–606 (1970).
3. M. Kawada, J. J. Bock, V. V. Hristov, A. E. Lange, H. Matsuhara, T. Matsumoto, S. Matsuura, P. D. Mauskopf, P. L. Richards, and M. Tanaka, "A rocket-borne observation of the far-infrared sky at high galactic latitude," Astrophys. J. **425,** L89–L92 (1994).
4. J. J. Bock, V. V. Hristov, M. Kawada, H. Matsuhara, T. Matsumoto, S. Matsuura, P. D. Mauskopf, P. L. Richards, M. Tanaka, and A. E. Lange, "Observation of [CII] 158-μm emission from the diffuse interstellar medium," Astrophys. J. **410,** L115–L118 (1993).
5. H. Matsuhara, M. Kawada, T. Matsumoto, S. Matsuura, M. Tanaka, J. J. Bock, V. V. Hristov, A. E. Lange, P. D. Mauskopf, and P. L. Richards, "A rocket-borne instrument for observations of near-infrared and far-infrared extended astrophysical emission," Pub. Astron. Soc. Jpn. **46,** 665–676 (1994).
6. For details of the LP100 filter, contact Perkin-Elmer, Norwalk, Conn. 06856.
7. S. Zwerdling and J. P. Theriault, "The low temperature transmittance of two far infrared LWP filters," Appl. Opt. **7,** 209–210 (1968).
8. A. E. Lange, E. Kreysa, S. E. McBride, P. L. Richards, and E. E. Haller, "Improved fabrication techniques for infrared bolometers," Int. J. Infrared Millimeter Waves **4,** 689–706 (1983).
9. R. Winston, "Light collection within the framework of geometrical optics," J. Opt. Soc. Am. **60,** 245–247 (1970).
10. M. G. Hauser, T. Kelsall, S. H. Moseley, Jr., R. F. Silverberg, T. Murdock, G. Toller, W. Spiesman, and J. Weiland, "The diffuse infrared background: COBE and other observations," in *Trends in Astroparticle Physics,* D. Cline and R. Peccei, eds. (World Scientific, Singapore, 1992), pp. 211–228.